

Valentine Anantharaj*¹, Georgy V. Mostovoy¹, Patrick Fitzpatrick¹, and Udaysankar Nair²¹Mississippi State University, Starkville, Mississippi²University of Alabama in Huntsville, Huntsville, Alabama

1. INTRODUCTION

Soil moisture estimates are considered as a valuable input for various environment models including weather forecasting, water management, agriculture, and forestry applications. Generally, the network of soil moisture observations is not dense (typically only few observation points are available within each state) enough to meet the spatial resolution requirements of these applications. Therefore, several approaches were developed to generate soil moisture fields. One approach utilizes Land Surface Model (LSM) offline simulations with a prescribed atmospheric forcing to produce high-resolution surface fields. The problem of adequate soil moisture initialization/specification in short-term numerical forecasting models was recognized about 10 years ago (Smith et al. 1994, Dirmeyer 1995).

Previous studies show a rather high sensitivity of predicted cloud properties and precipitation amounts to relatively small changes in initial soil moisture patterns at regional scale (e.g. Grasso 2000, Cheng and Cotton 2004). Although a remarkable progress has been done in this area in recent years, there is still lack of knowledge about soil moisture impact on the development of clouds and precipitation. Therefore, the objective of this research was to investigate sensitivity of regional weather forecasts to different initialization of soil moisture.

2. STUDY AREA AND MODELS SETUP

The research results discussed in this report were obtained over two regions with different dominant vegetation and soil types. One region was selected over the Mississippi Delta with dominant Dryland/Cropland/Grassland Mosaic vegetation

type and clayey soils. For convenience, this region was represented by a rectangular and denoted by letter A in Fig. 1. Other region with dominant Evergreen Needleleaf Forest vegetation category and sandy/loamy soils was located to the south from the Mississippi Delta. This region is shown in Fig. 1 by letter B.

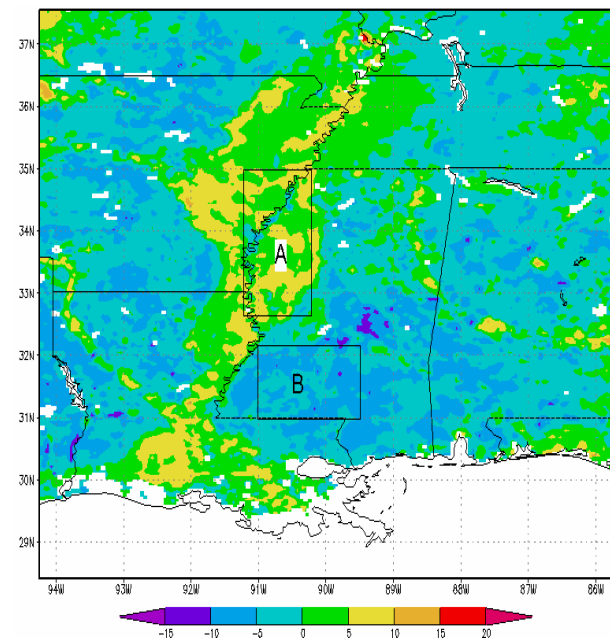


Figure 1. Difference between initial soil moisture fields (Noah/LIS – NAM 12-km) shown in Fig. 2 within WRF computational domain. Rectangles A and B stand for regions used for atmospheric response comparisons between WRF runs performed with Noah/LIS and NAM 12-km (considered as control run) initial soil moisture. Note that soil moisture from Noah/LIS is overestimated (positive difference of Noah/LIS minus NAM 12-km) over region A and underestimated over region B in comparison with NAM 12-km initial fields.

The **Noah** LSM (Ek et al., 2003) available within the state-of-the-art Land Information System (LIS) developed at NASA Goddard Space Flight Center (Peters-Lidard et al., 2004, Kumar et al., 2006) was configured at 0.05°x0.05° latitude-longitude resolution (approximately 5x5 km²) over a domain covering the state of Mississippi and adjacent

*Corresponding author address: Georgy V. Mostovoy, Mississippi State Univ., GeoResources Institute, Starkville, MS, 39759; e-mail: mostovoi@hpc.msstate.edu

states. Location of the Noah/LIS computational domain is shown in Fig. 1. The LIS provides a rather flexible tool for unified specification of land topography, soil and vegetation parameters, and running various LSMs either regionally or globally.

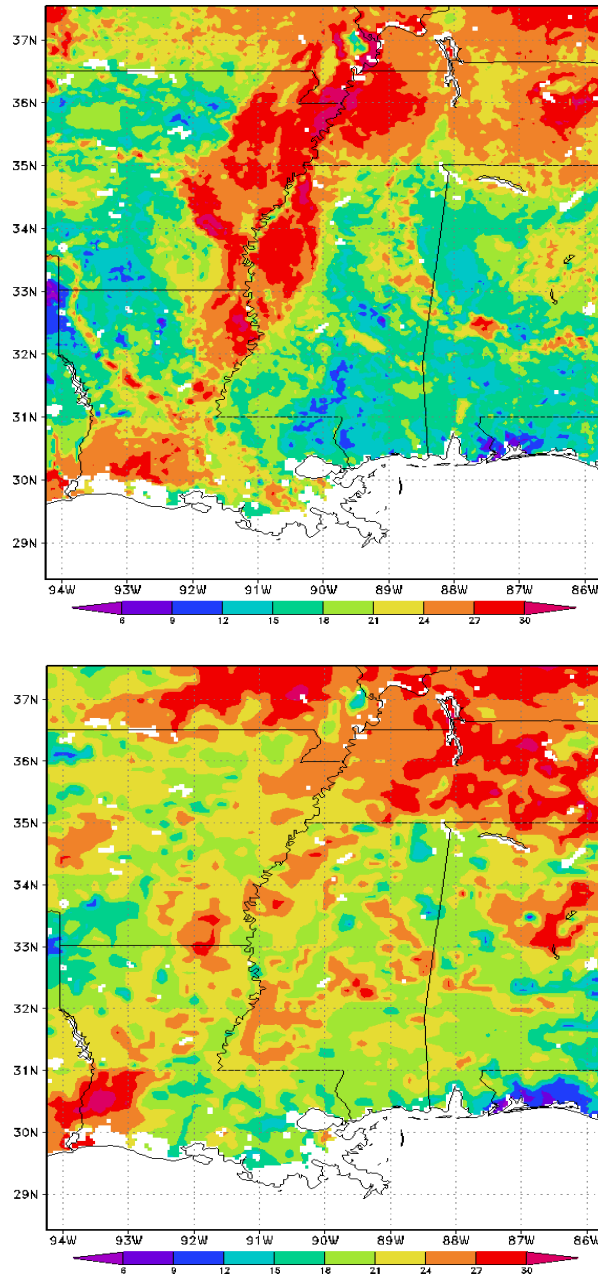


Figure 2. Examples of top 0-10 cm soil moisture initial distribution within WRF computational domain (07/01 2006 00 UTC). Distribution produced from Noah/LIS 5-km retrospective run (upper frame) and from NAM 12-km analysis (lower frame)

The Noah LSM (version 2.7.1) was used for moisture simulations with 4 standard soil layers

stretching from the surface to 2-m depth. The soil texture was represented by CONUS-SOIL (Miller and White, 1998) data based on USDA STATSGO database. The geographical distribution of STATSGO soil classes within the Noah/LIS integration domain is shown in Fig. 3. Only five texture classes (sandy loam, silt loam, silty clay loam, silty clay, and clay) are observed over the model domain, as shown in Fig. 3. Clay soils (silty clay loam, silt clay, and clay) depicted in magenta, yellow, and gray colors are dominant over the Delta with a small quantity of sandy soils observed mainly along the Mississippi River (see Fig. 3). Sandy soils (sandy loam and silt loam) prevails to the east and west from the Delta, so there is a clear contrast of the soil texture exists between the Delta and adjacent territories. The vegetation/land use description was based on 13 land cover classification types developed at the University of Maryland.

For retrospective simulations the LIS framework supports various atmospheric data sets such as GLDAS, GOES, NLDAS, ECMWF, and others with different levels of spatial and temporal resolution. The atmospheric input (forcing) into the LIS involves the following surface variables: air temperature and water vapor content, pressure, components of the wind, downward fluxes of solar and longwave radiation, and rain- snowfall rates. In the present study North American Land Data Assimilation System (NLDAS) atmospheric data were used to force the Noah LSM model. The NLDAS forcing project was described in detail by Cosgrove et al. (2003). NLDAS hourly fields cover the CONUS region and some adjacent regions of Canada and Mexico with $0.125^\circ \times 0.125^\circ$ latitude-longitude resolution (approximately 15 km grid spacing). They are available online from the end of 1996 until the present. The Noah/LIS runs were performed using NLDAS forcing spanning the period from January 2004 to the end of the year 2006.

An advanced version 2.2 of the Weather Research and Forecasting (WRF) model (Skamarock et al., 2006) was used to perform two set of thirty 72-h regional forecasts. The WRF model was configured with horizontal spacing of 4 km having 31 vertical levels. Each forecast was started every other day spanning a period June-July 2006. The forecast period from 25 hr to 72 hr was used for comparison purposes.

One set of forecasts was initialized from NAM 12-km analysis and these forecasts were considered

as control runs. Other set of regional forecasts was performed with the same initial conditions as in control run, except for the soil moisture fields were substituted by those produced by Noah LSM retrospective simulations using LIS. Comparisons between two sets of the WRF forecasts were focused over the central part of the integration domain (the Mississippi Delta) where a persistent positive difference of about 3-5 % in volumetric content units was observed between Noah/LIS and control SM initial fields. The MS Delta region used for the comparison purposes was approximated by the rectangle, which is depicted in Fig. 1 by the letter A. Additional comparisons were performed over the forested region (shown as rectangle denoted by the letter B in Fig. 1), which was located to the south from the Delta and where the Noah/LIS simulations produced a consistently lower soil moisture (by 3-5% of volumetric content) in comparison with NAM 12-km analysis fields.

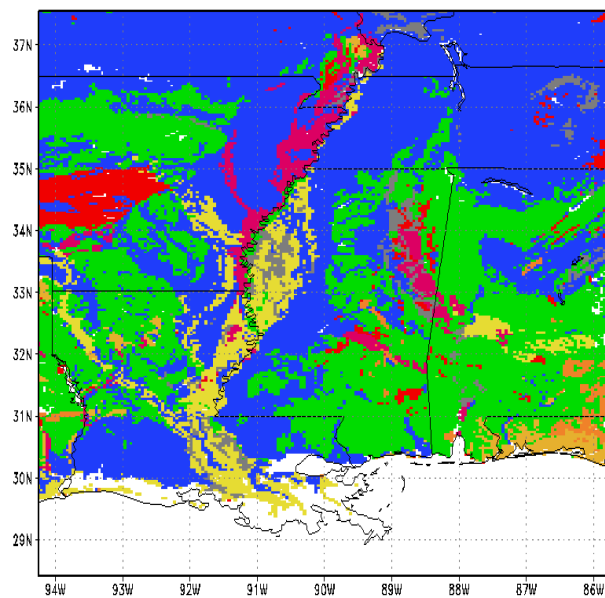


Figure 3. Geographical distribution of STATSGO soil types (a) and USGS Land Use indexes (b) within WRF integration domain. Dominant types/indexes within WRF 4-km grid mesh are depicted. Water – white. **Soil types legend:** Sand (dark yellow), Loamy Sand (orange), Sandy Loam (green), Silt Loam (blue), Loam (red), Silty Clay Loam (gray), Silty Clay (magenta), and Clay (yellow).

It is important to note that both the WRF model and the Noah/LIS use the same classification scheme and the same STATSGO data base to describe spatial variability of soil types observed within the computational domain (Fig. 3).

Conversely, the USGS land use (vegetation) classification scheme is used by the WRF model to describe surface-atmosphere interactions and this scheme differs from that used in Noah/LIS simulations (the UMD land use scheme). This difference is a major reason for soil moisture spatial patterns difference between Noah/LIS and NAM 12-km fields, illustrated by Fig. 1.

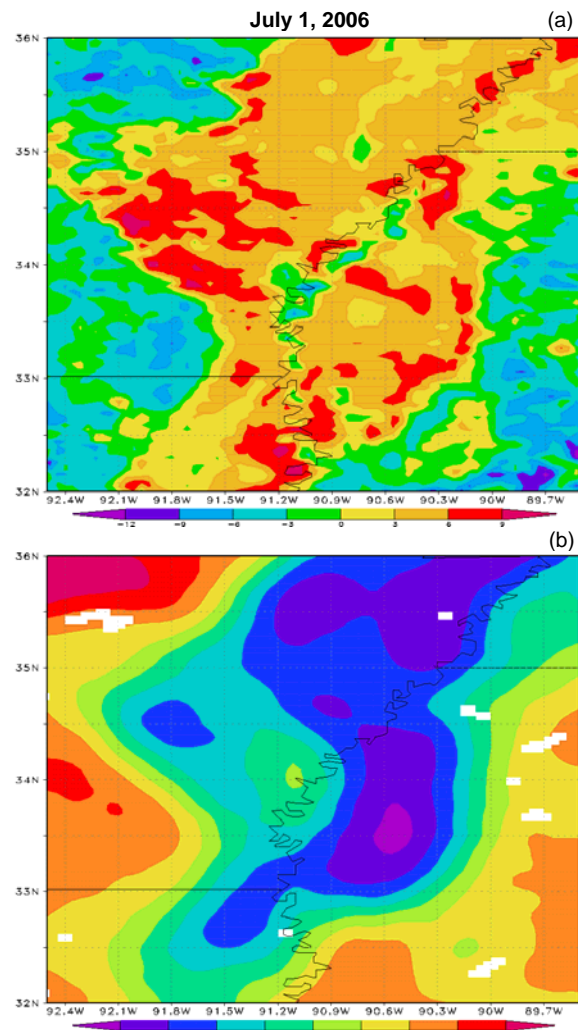


Figure 4. Geographical distribution of top 0-10 cm soil moisture difference (Noah/LIS – Control) [a] and mean vegetation fraction [b] over Mississippi Delta for July.

3. RESULTS

Noah/LIS runs were performed using NLDAS forcing spanning the period from January 2004 to the end of the year 2006. Figure 2 shows a typical example of the soil moisture geographical distribution simulated by the Noah/LIS. Close association of simulated top 0-10 cm soil moisture (upper frame in Fig. 2) spatial patterns with those

of soil types shown in Fig. 3 is apparent. Specifically, areas of relatively low soil moisture content coincide with regions of “sandy” and “loamy” soil types (green and blue colors in Fig. 3). Conversely, areas of relatively high moisture correspond to clay soil types indicated by gray, magenta and yellow colors in Fig. 3.

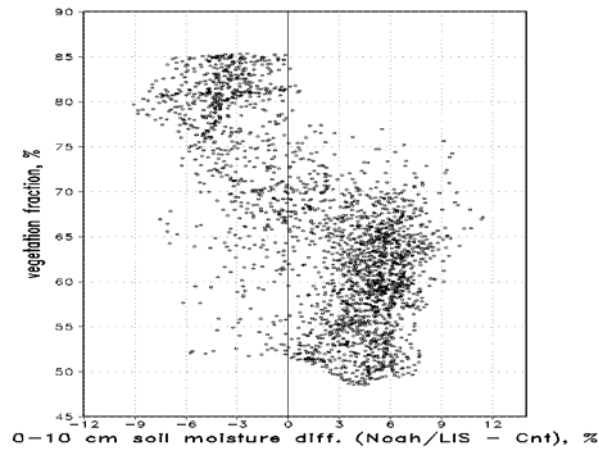


Figure 5. Scatterplot between top 0-10 cm soil moisture difference (Noah/LIS – Control) and mean vegetation fraction depicted in Fig. 4.

Before describing results of sensitivity experiments with the WRF model, it is important to note that spatial patterns of top 0-10 cm soil moisture difference between Noah/LIS fields and NAM 12-km analysis are related to those of the vegetation fraction (see Figs. 4 and 5). Noah/LIS soil moisture fields show rather persistent increase over the MS Delta (region A) and decrease over the B region as compared with NAM 12-km soil moisture fields. These features are illustrated by Figs. 6 and 7, which depicted time series of spatial mean and standard deviation for top 0-10 soil moisture content over selected regions A and B. Therefore, it might be expected that both surface layer and atmospheric boundary layer responses over these regions will be similar, but having different signs.

3.1 Surface layer response

Above mentioned differences between Noah/LIS and NAM 12-km initial soil moisture fields result in corresponding changes in water vapor vertical flux within the surface layer as illustrated by Fig. 8. Indeed, there is a rather persistent positive difference of surface water vapor flux averaged over the Mississippi Delta (region A) between Noah/LIS and control WRF runs. The negative difference of the surface water vapor flux is

observed over the region B (see Fig. 8). As expected, an average soil moisture increase over the region A results in reduced skin/surface and near-surface air temperatures as shown in Fig. 9. An opposite tendency is observed over the region B where soil moisture decrease as compared with control runs results in elevated skin/surface and near-surface air temperatures as shown in Fig. 10. Maximum increase or decrease in the water vapor flux and related temperatures changes is observed around the midday.

3.2 Atmospheric boundary layer response

Surface anomalies of water vapor flux and temperatures mentioned in the previous section, which caused by different soil moisture initializations propagate upward from the surface leading to moistening/drying and heating/cooling of the atmospheric boundary (mixing) layer during day hours. Figure 11 shows differences of water vapor mixing ratio and potential temperature averaged over the Mississippi Delta between WRF initialized with the Noah/LIS soil moisture and control runs spanning a period from July 12 to July 31, 2006. Only contours exceeding ± 1 g/kg and ± 0.5 K are shown in Fig. 11 for water vapor mixing ratio and potential temperature differences, respectively. Major changes occur within and above mixing layer during afternoon hours as illustrated by Fig. 12. Increase of soil moisture results in a mixing layer that is nearly 2 g/kg moister and 2 K cooler than in the control WRF simulation during July 29, 2006. At same time the mixing layer becomes thinner than in the control run. Note that over the region where soil moisture is lower than in control run (see region B in Fig. 1) the mixing layer responded in an opposite way: it becomes drier and warmer in comparison with the control run (Figures not shown). All these changes in the mixing layer structure are in agreement with previous numerical simulations of local atmospheric boundary layer response to soil moisture positive anomalies (e.g. Chen and Avissar 1994, Golaz et al. 2001).

Manifestation of the changes in the mixing layer structure also depends on atmospheric thermodynamical properties (vertical profiles of water vapor mixing ratio and potential temperature) which experienced regular variability with a typical period of 10-14 days over regions selected for analysis. This variability is modulated by large- and planetary-scale atmospheric dynamics leading to periodic changes of atmospheric flow.

Indeed, quasi-regular changes in v-component of the wind averaged over the region A are produced by control runs. For example, southerly winds bring moister and warmer air than northerly winds (data not shown).

Layer-averaged response of the lower troposphere water vapor mixing ratio and potential temperature to the changes in initial soil moisture over the region A is shown in Figs. 13 – 14.

Finally, there are no substantial or consistent changes in cloud fraction (Figs. 15 and 16) and precipitation amount (data not shown) between WRF simulations with Noah/LIS soil moisture and control runs.

4. SUMMARY

- ❑ Soil moisture within top 0-10 cm layer simulated with the Noah/LIS model retrospective runs show persistently higher values over the MS Delta region (and lower values over forested areas to the south) as compared with that of the NAM 12-km analysis fields. Spatial patterns of the initial soil moisture fields simulated by the Noah/LIS retrospective runs are more closely related to vegetation fraction, soil texture, and land use category than soil moisture fields from the NAM analysis.
- ❑ Comparisons of 30-day parallel forecasts with the WRF model having different soil moisture initialization have shown that an initial increase/decrease of soil moisture over regions with a typical size of $1^{\circ}\times 1^{\circ}$ latitude-longitude resulted in a consistent linear and locally-concentrated response within the atmospheric boundary layer leading to it cooling/warming and moistening/drying during day hours. This fact is an agreement with previous soil moisture sensitivity studies (e.g. Golaz et al. 2001), which reported the similar response of the atmospheric boundary layer to increase/decrease of soil moisture.
- ❑ No substantial changes in shallow clouds and precipitation amounts averaged over two adjacent regions (A and B) were observed between WRF runs with initial Noah/LIS and NAM soil moisture fields.

5. ACKNOWLEDGMENTS

The research is sponsored by the NASA-funded GeoResources Institute at Mississippi State University, Mississippi State, MS. We appreciate timely consultations provided by the LIS Helpdesk (Drs. Sujay Kumar and Yudong Tian). We acknowledge an effort of the USDA Natural Resources Conservation Service for maintaining the SCAN data webpage.

6. REFERENCES

- Chen, F. and R. Avissar, 1994: Impact of land-surface moisture variability on local shallow convective cumulus and precipitation in large-scale models. *J. Appl. Meteor.*, **33**, 1382-1401.
- Cheng, W.Y.Y. and W. Cotton, 2004: Sensitivity of a cloud-resolving simulation of the genesis of a mesoscale convective system to horizontal heterogeneities in soil moisture initialization. *J. Hydrometeor.*, **5**, 934-958.
- Cosgrove, B.A. and Coauthors, 2003: Real-time and retrospective forcing in the North American Land Data Assimilation System (NLDAS) project. *J. Geophys. Res.*, **108**, D22, 12pp.
- Dirmeyer, P.A., 1995: Problems in initializing soil wetness. *Bull. Amer. Meteor. Soc.*, **76**, 2234-2240.
- Ek, M.B., K.E., Mitchell, Y., Lin, E., Rogers, P., Grunmann, V., Koren, G., Gayno and J.D., Tarpley, 2003: Implementation of NOAH land surface model advances in the National Centers for Environmental Prediction operational mesoscale Eta model. *J. Geophys. Res.*, **108**, D22, 16pp.
- Golaz, J.-C., H., Jiang and W. Cotton, 2001: A large-eddy simulation study of cumulus clouds over land and sensitivity to soil moisture. *Atmos. Research*, **59-60**, 373-392.
- Grasso, L.D., 2000: A numerical simulation of dryline sensitivity to soil moisture. *Mon. Wea. Rev.*, **128**, 2816-2834.
- Kumar, S.V. and Coauthors, 2006: Land Information System – An interoperable framework for high resolution land surface modeling. *Environmental Modelling and Software*, **21**, 1402-1415.
- Miller, D.A. and R.A. White, 1998: A conterminous United States multi-layer soil characteristics data set for regional climate and hydrology modeling. *Earth Interactions*, **2**, 1-26.
- Peters-Lidard, C.D., S.V., Kumar, Y. Tian, J.L., Eastman and P.R. Houser, 2004: Global Urban-Scale Land-Atmosphere Modeling with the land Information System. In Proc. 84th AMS Annual Meeting, Seattle, WA, 13 pp., 11-15 Jan., 2004.

- Skamarock, W.C. and coauthors, 2006: A description of the Advanced Research WRF version 2. *NCAR Technical Note/TN-468+STR*, NCAR, Boulder, CO, 88pp.
- Smith, C.B., M.N., Lakhtakia, W.J., Capehart and T.N., Carlson, 1994: Initialization of soil-water content in regional-scale atmospheric prediction models. *Bull. Amer. Meteor. Soc.*, **75**, 585-593.

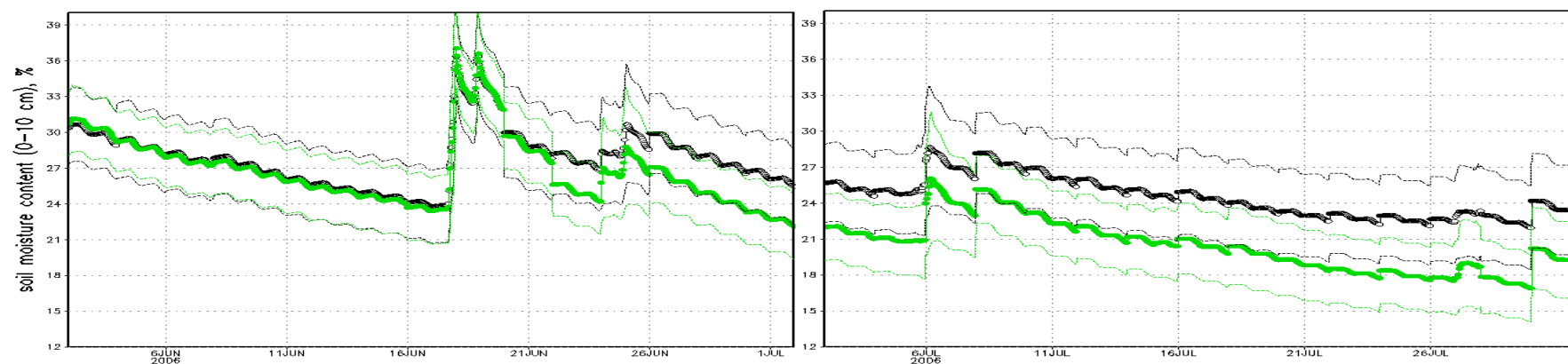


Figure 6. Time series of the top 0-10 cm soil moisture content averaged over domain located within Mississippi Delta Region (domain location is depicted in Fig. 1 by letter A). Control run (green) and run with Noah/LIS initial soil moisture (black). Notice that Noah/LIS produce systematic/persistent over-moistening over the Delta (region A) during the second half of June and all July. Dashed lines indicated standard deviation limits.

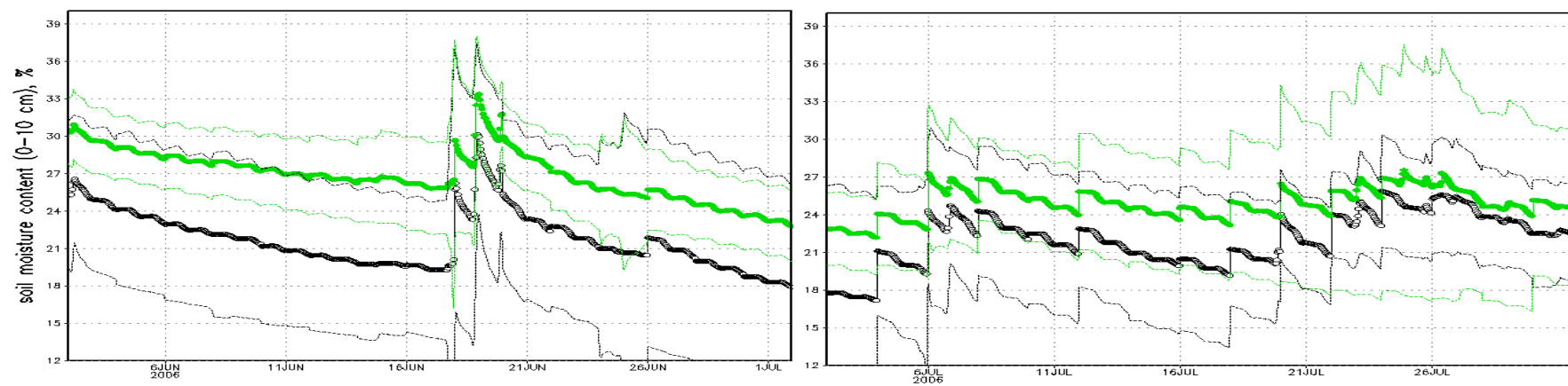


Figure 7. The same as in Fig. 5, but for domain B shown in Fig. 1.

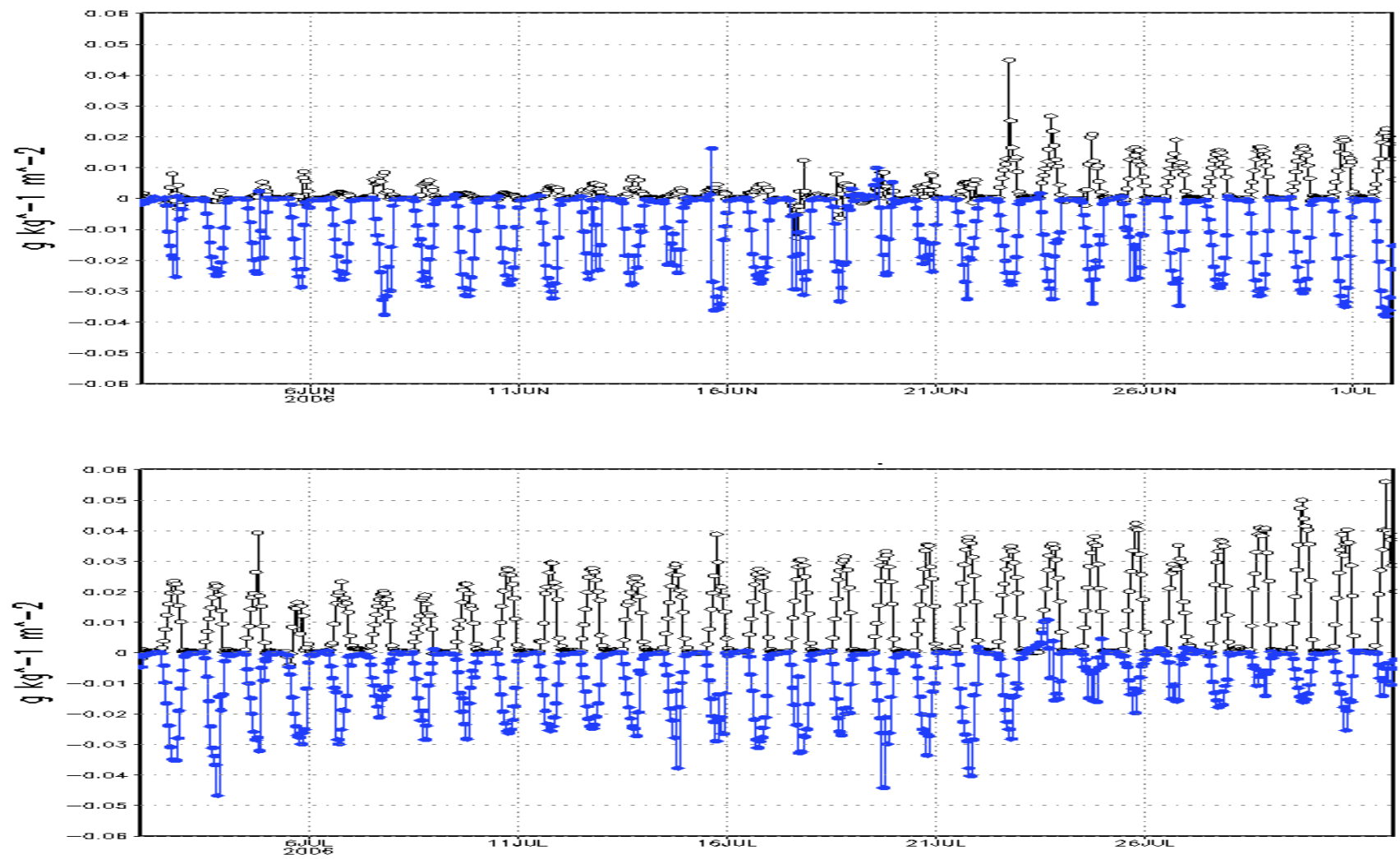


Figure 8. Time series of the water vapor surface flux difference between WRF runs with Noah/LIS initial soil moisture and control simulations. Values are averaged over domain A (black line) and B (blue line). See Fig. 1. for domains locations.

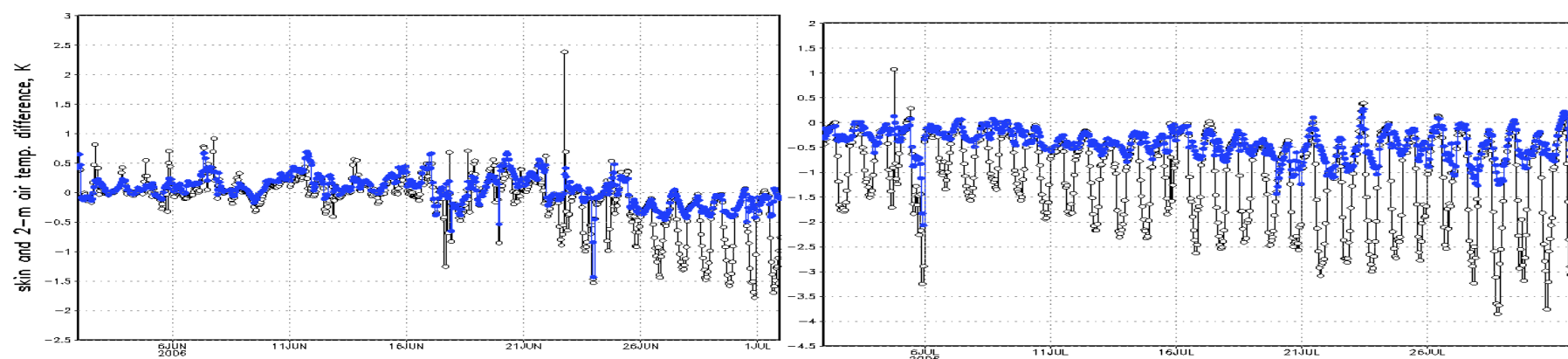


Figure 9. Time series of the temperature difference between WRF runs with Noah/LIS initial soil moisture and control simulations. Values are averaged over domain located within Mississippi Delta Region (domain A in Fig. 1). Skin/surface temperature (open circles) and 2-m air temperature (blue filled circles).

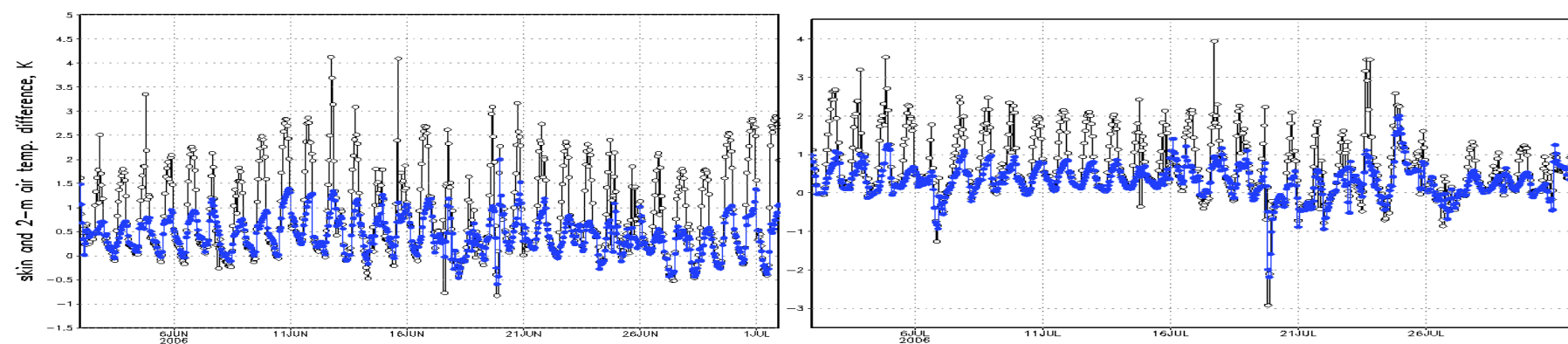


Figure 10. The same as in Fig. 9, but for domain B shown in Fig. 1.

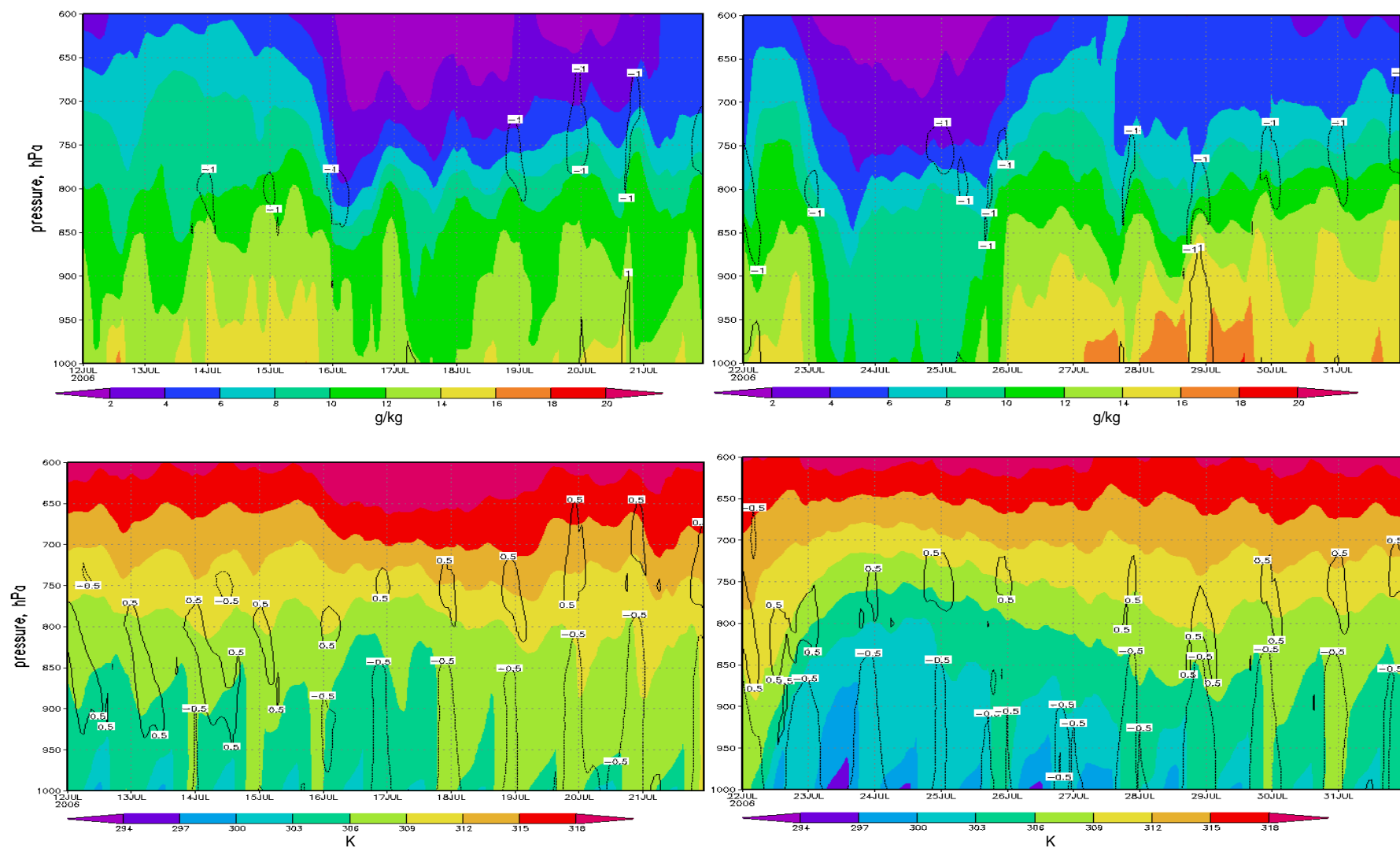


Figure 11. Time series of hourly difference (averaged over the MS Delta /region A/) between WRF runs with Noah/LIS and control (NAM 12 km) soil moisture are shown by contours for total water vapor mixing ratio (upper row) and for potential temperature (lower row). Color shading stands for total water vapor mixing ratio (upper row) and potential temperature (lower row) produced from control runs. July 12 to July 31, 2006.

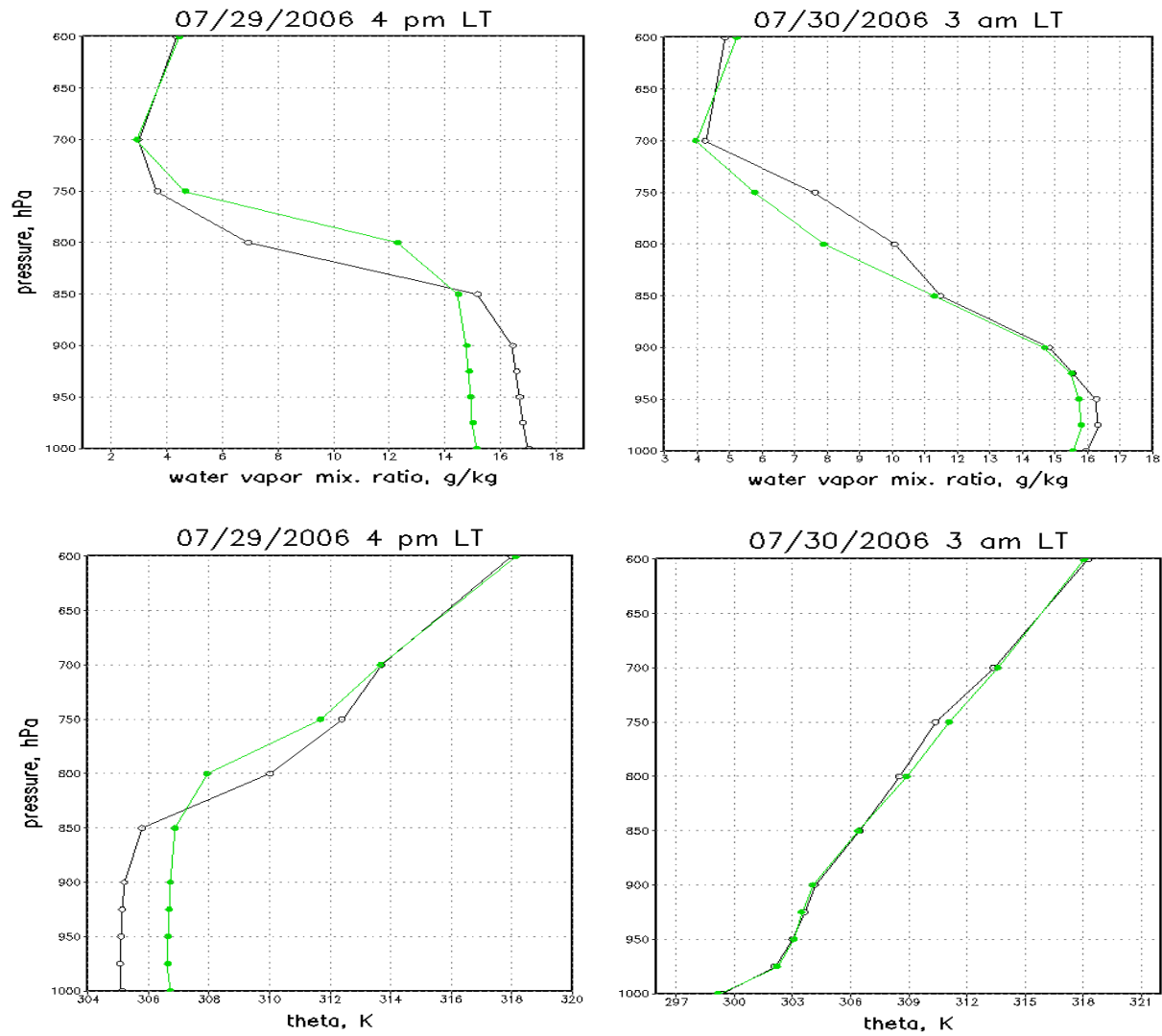


Figure 12. Examples of typical changes in total water vapor mixing ratio and potential temperature vertical profiles during day and night hours. Green color stands for control run and black for the WRF run with Noah/LIS soil moisture. Values are averaged over Mississippi Delta (region A in Fig. 1).

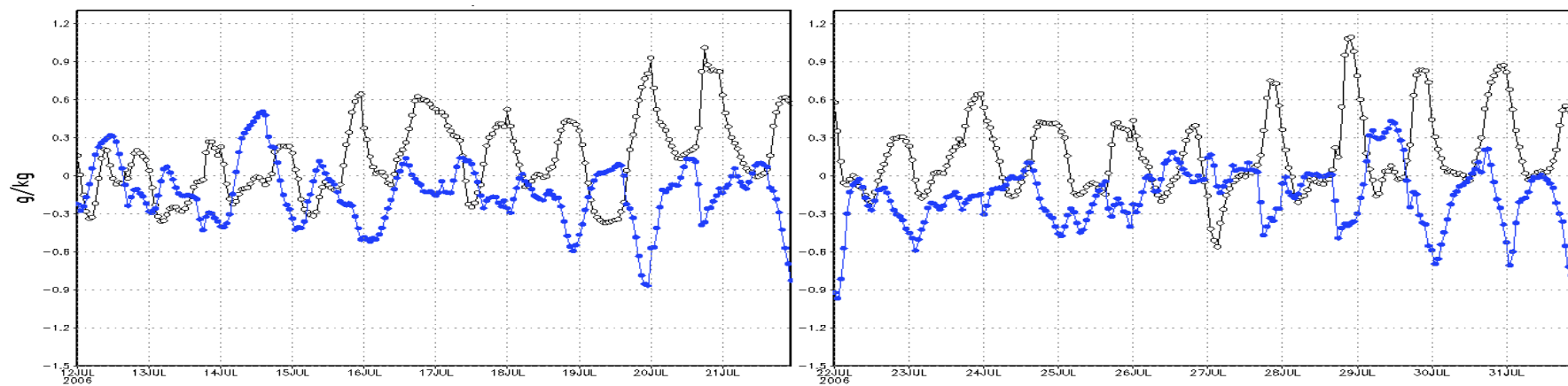


Figure 13. Time series of water vapor mixing ratio hourly difference (averaged over the MS Delta /region A/) between WRF runs with Noah/LIS and control (NAM 12 km) soil moisture. Values are averaged within 1000-850 hPa (black open circles) and within 850 – 700 hPa (blue filled circles) layer. Period from July 12 to July 31, 2006.

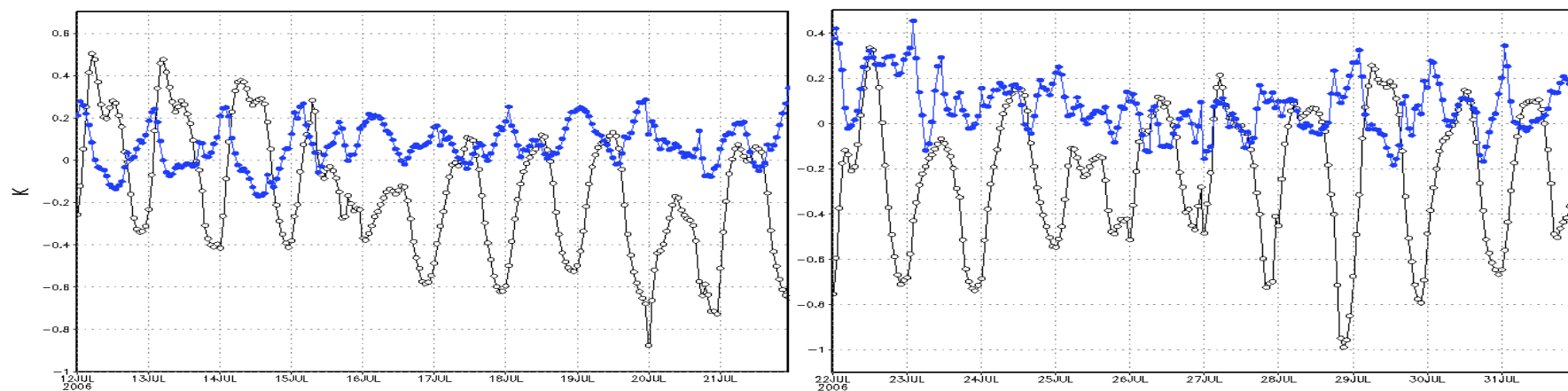


Figure 14. The same as in Fig. 14, but for potential temperature.

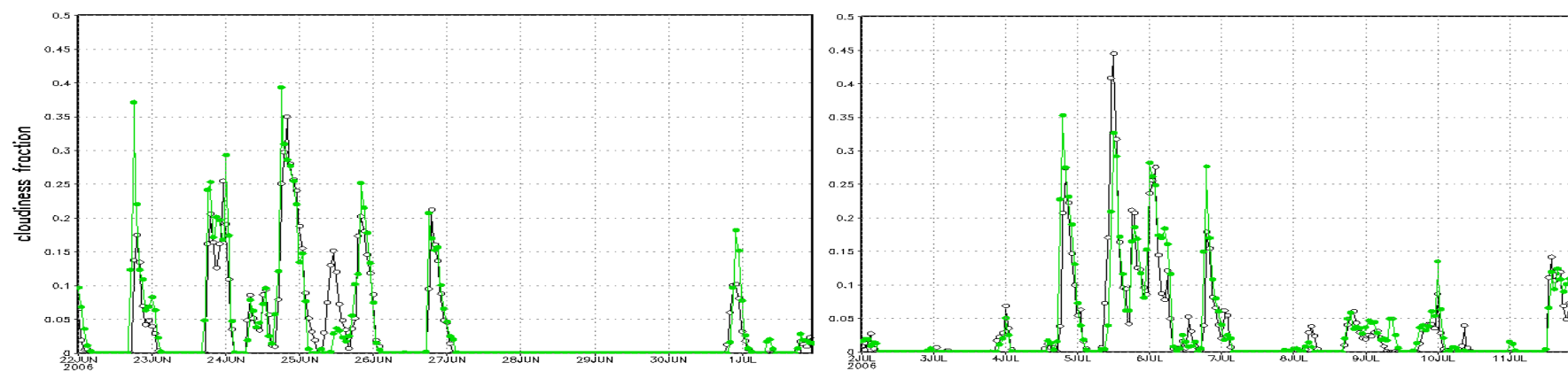


Figure 15. Time series of cloud fraction from control (green) and Noah/LIS (black) runs. Values were averaged over the MS Delta (region A in Fig. 1c) and within 850 – 700 hPa layer. Period from June 22 to July 12, 2006.

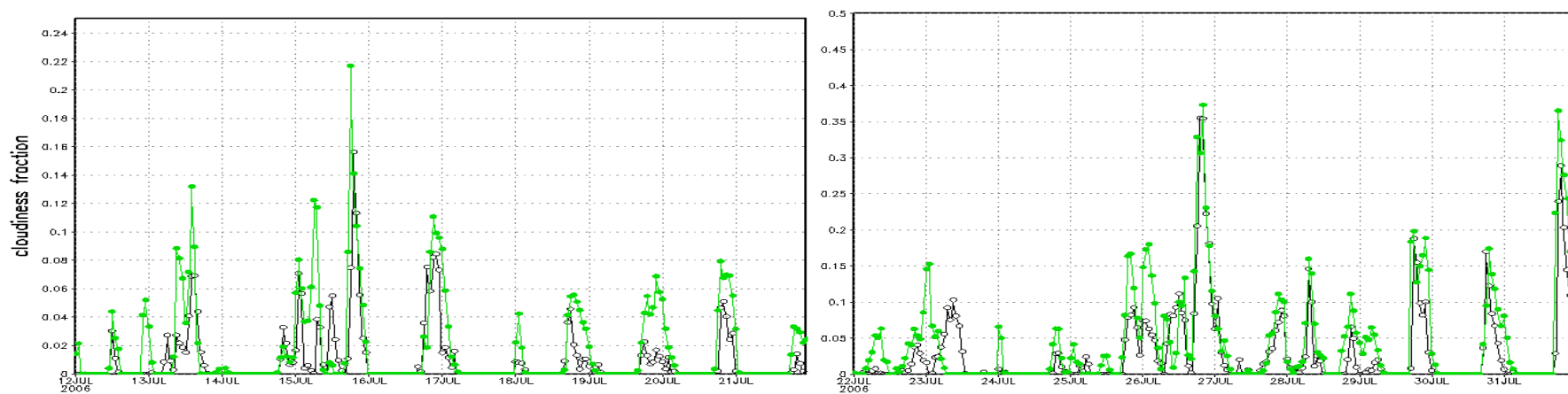


Figure 16. The same as in Fig. 16, but for period from July 12 to July 31, 2006.